Automated mineralogical profiling of soils as an indicator of local bedrock lithology: a tool for predictive forensic geolocation

Duncan Pirrie[a,d], Daniel E. Crean[b], Allan J. Pidduck[b], Timothy M. Nicholls[b], Roy P. Awbery[b], Robin K. Shail[c]

[a]Helford Geoscience LLP, Trelowarren Mill Barn, Mawgan, Helston, Cornwall, TR12 6AE, UK

[b]AWE Plc, Aldermaston, Reading, RG7 4PR, UK

[c]Camborne School of Mines, University of Exeter, Penryn Campus, Penryn, Cornwall, TR10 9FE, UK

[d]School of Applied Sciences, Faculty of Computing, Engineering and Sciences, University of South Wales, Glyntaf, Pontypridd, Rhondda Cynon Taff, CF37 4AT, UK

ABSTRACT

The use of soil evidence to identify an unknown location is a powerful tool to determine the provenance of an item in an investigation. We are particularly interested in the use of these indicators in nuclear forensic cases, whereby identification of locations associated with for example, a smuggled nuclear material, may be used to indicate the provenance of a find. The use of soil evidence to identify an unknown location relies on understanding and predicting how soils vary in composition depending on their geological / geographical setting. In this study, compositional links between the mineralogy of forty soils and the underlying bedrock geology were established. The soil samples were collected from locations with broadly similar climate and land use across a range of geological settings in a 'test bed' 3500 km^2 area of South West England. In this region, the soils formed through chemical weathering of the bedrock, representing a worst case for

this type of forensic geolocation due to the high degree of alteration of the parent rock during soil formation. The mineralogy was quantified using automated SEM-EDX analysis. The soil mineralogy and texture are consistent with the underlying geology as indicated by regional-scale geological mapping.

Keywords: soil forensics, provenancing.

Introduction

It is widely recognised that soil is a useful class of trace evidence which can be used to test a possible association between a geographical location and material recovered from, for example, footwear, clothing, vehicles and objects used during an offence (e.g. Bull et al., 2006; Pirrie and Ruffell, 2012). In general, most published forensic soil science studies have addressed the use of soil as an evidential tool, testing an association between an object and a known location through comparative analysis (Fitzpatrick et al., 2009). However, soil analysis can also be used to attempt to identify unknown locations based on the soil characteristics (Bowen and Craven, 2013; Lark and Rawlins, 2008; Owens et al., 2016). This use of soil trace evidence to determine the geographic position of otherwise unknown locations can be referred to as predictive geolocation (Pirrie et al., 2017) and is of increasing interest to the forensic geoscience community (e.g. Stern et al., 2019; Caritat et al., 2019).

One aspect of our interest in predictive geolocation relates to its potential to determine the geographic source (provenance) of an item in a nuclear forensic investigation (Mayer et al., 2012). These scenarios involve the discovery or interdiction of nuclear material outside regulatory or institutional control, such as so-called ‘nuclear smuggling’ cases (Wallenius et al., 2006; Mayer et al., 2015). In these investigations, there may be a wide range of potential sources of the material, (e.g. facilities which have processed the particular type of material), and therefore the potential to constrain the possible origins of a find through predictive geolocation analysis would be of great value in establishing the provenance of a found material.

This is complementary to the types of analysis which fall under the field of nuclear forensic science (Keegan et al., 2016), which relate to the properties of the material itself, such as the identification of particular processes through the evaluation of signature chemical properties of the material.

Predictive geolocation analysis relies on signatures accumulated from the environments to which a nuclear material has been exposed during production, transport and storage; both before and after institutional control was lost. Packing and repackaging of materials may introduce a number of internal interfaces where materials from different environments may accumulate. These environmental signatures may include natural materials such as soils and dusts, to which forensic soil geolocation analysis techniques can be applied to indicate location(s) associated with the sample.

For this predictive geolocation analysis to be practical, it is necessary to select key parameters which can be measured in a realistic (short) timescale for use in an investigation, and which have a high degree of specificity in indicating an unknown location. Owing to the wide availability of spatial geological reference datasets (e.g. from national geological surveys), indicators related to the underlying lithology at a location are useful in this context (Pirrie et al., 2013). Determination of the likely source geology from soil analysis would allow an investigation to be focussed to areas where this setting is known to occur. For this approach to have forensic validity, the relationship between soil mineralogy and underlying geology has to be established. Soil-forming processes can profoundly alter the composition of the parent material depending on environmental conditions, and therefore there is a need to understand the specificity with which lithological signatures could be detected in a range of soil forming environments.

In this paper we present a systematic study of the relationship between the underlying geology and soil mineralogy in a geologically varied 3500 km^2 area of SW England. The area provides a ‘test bed’ with a variety of well documented major rock types and settings. Soils within the area are mainly mature loams, developed through chemical weathering and human management. This represents an advanced state of alteration of the underlying rock and therefore a high potential for disturbance of the mineralogical signatures linking the soil to the associated bedrock. Automated mineralogy based on scanning electron microscopy was used as a rapid method for characterisation the mineralogy and texture of the soils. This tests the link between rapidly measureable soil characteristics (in this case mineralogy) and widely available geological datasets, such that an indication of potential geological settings could be provided from an unknown soil sample in an investigation.

Overview of Study Area

In this study 35 geographical locations over an area of approximately 3500 km^2 in Cornwall and Devon, SW England, UK were selected for soil sampling (Fig. 1, Table 1). Factors such as variations in climate and land-use were minimised as far as possible, such that the dataset allows the significance of the underlying bedrock geology as the main control on soil mineralogy to be tested. All of the sampling locations would also have had surface superficial sediments present mantling the bedrock geology to variable extents.

The selected sampling area whilst geologically varied, shows the repetition of a number of major rock types, and samples from these were taken to test discrimination between soils developed on different age units composed of the same dominant rock types. SW England has also been a recent focus for baseline environmental and geochemical surveys based on both airborne datasets and regional surface soil and sediment sampling programmes (Beamish, 2015; Kirkwood et al., 2016).

Geology

SW England is an Upper Palaeozoic massif whose bedrock geology, in common with much of western Europe, was strongly influenced by the late Palaeozoic Variscan mountain-building episode (Shail and Leveridge, 2009). The near-surface geology is dominated by Devonian and Carboniferous metasedimentary rocks (Fig 1.). Other significant features include associated minor basic intrusive / extrusive igneous rocks, a major granite batholith which was emplaced in the Early Permian, and the Lizard Complex, which includes partially serpentinised mantle peridotites, gabbros and high-grade metamorphosed mafic igneous rocks. Devonian and Carboniferous successions occur in six east-west trending sedimentary basins (Leveridge, 2011; Leveridge and Shail, 2011a, b). These formed during rifting which resulted in the formation of a passive margin and associated oceanic lithosphere. Sedimentation in the Gramscatho and Culm basins continued during the early stages of the Variscan continental collision (Leveridge, 2011; Leveridge and Shail, 2011a). The Looe Basin includes non-marine sandstones and mudstones (Leveridge, 2011) but, more generally, the basin successions comprise mudstones and sandstones, along with minor limestones and cherts, deposited in shallow to deep-marine environments (Leveridge and Shail, 2011b). Rift-related mafic igneous rocks (basalts, dolerites and gabbros) are locally important constituents of the basin fills and sedimentary exhalative (SedEx) and volcanic massive sulphide (VMS) mineralisation styles locally occur (Benham et al., 2005). The Lizard Complex includes partially serpentinised mantle peridotites, gabbros and high-grade metamorphosed mafic igneous rocks; it represents a fragment of the oceanic lithosphere (an ophiolite) formed during rifting and also includes small areas of high-grade continental metamorphic rocks.

Variscan continental collision brought about deformation and low-grade regional metamorphism of all of the basinal successions (Shail and Leveridge, 2009). Consequently the rocks are variably thrust-faulted and folded and one or more cleavages are developed. Quartz veins, precipitated from metamorphic fluids, are ubiquitous and locally associated with precious metal mineralisation. Continental collision continued until the latest Carboniferous, when it was followed by a NNW-SSE extensional regime which persisted through most of the Early Permian. This extension led to the development of post-Variscan Permian ‘red-bed’ sedimentary basins (Edwards et al., 1997) and voluminous post-collisional felsic magmatism. The principal expression of the latter is the Cornubian Batholith which comprises a variety of granite types and is associated with rhyolite / microgranite dykes known locally as ‘elvans’ (Simons et al., 2016). Host rocks within 1 km or so of the batholith margins exhibit contact metamorphism. The granites, elvans and their surrounding host rocks are cut by extensional fault systems hosting Early-Mid-Permian polymetallic W-Sn-Cu-As-Pb-Zn magmatic-hydrothermal mineralisation, the working of which has resulted in substantial areas of metal-contaminated made ground throughout the region (Pirrie et al., 2003). A subordinate Mid-Triassic fault-controlled epithermal mineralisation episode, associated with the migration of basinal brines from ‘red-bed’ basins, resulted in localized Pb-Zn-barite mineralization (Simons et al., 2011).

The Quaternary geological history of SW England is dominated by repeated intervals of periglacial climates and warmer inter-glacials. Although some authors have speculated on the possibility of small cirque glaciers (Harrison et al., 1998), there is no evidence for significant glaciation throughout the region during the repeated cold climate intervals of the Quaternary. Instead the bedrock geology was influenced by periglacial processes with down-slope mass wasting of the local bedrock units. These locally derived periglacial sediments are referred to as “head deposits” and typically thicken into valleys. Along the north coast marine-derived carbonate blown sand deposits are locally developed as dune sand systems. Flooded steep sided valley systems known as rias, now forming major estuaries, are developed along the south coast (e.g. the Helford, Fal, Fowey and Tamar estuaries) along with smaller scale systems on the north coast (Hayle, Gannel and Camel estuaries). These estuaries have received significant volumes of contaminated mine waste as a result of the historical mining activity in the region (Pirrie and Shail, 2018).

For the purposes of presentation and analysis of results, six broad lithological groupings were identified from geological maps into which the sampling locations were assigned. These were granitic (samples 1, 3, 10, 17, 20 and 34), mafic-igneous (samples 2, 12, 15, 22, 32, 35), metamorphic (samples 4, 5, 14, 16), metamorphosed mudstone (samples 6, 7, 8, 13, 18, 19, 21, 23, 24, 26, 27, 28, 29), metamorphosed sandstone (samples 9, 11, 25) and Carboniferous sedimentary (samples 30, 31 and 33).

Geography, climate and soils

Despite the historical mining industry throughout the region, Cornwall and Devon are today predominantly rural environments dominated by agricultural land use. Lower lying areas are typically underlain by the Devonian and Carboniferous metasedimentary rocks whilst the granites underlay upland moorland which has an elevation of up to 621 m on Dartmoor. The region has an oceanic climate, with a small range in annual mean temperature between approximately 6ºC (winter) and 16ºC (summer), mild winter temperatures and among the highest wind speeds in the United Kingdom. Winters are wet and summers dry with annual precipitation totals of 900–1,000 mm at the coast, although annual precipitation increases inland, to up to 2,000 mm on the granite moorland (Kosanic et al., 2014).

According to the available soil classification schemes, the soil types present show relatively little variation within the studied area (www.landis.org.uk/soilscapes). The majority of the Devonian and Carboniferous metasedimentary rocks are overlain by acidic loamy soils, slightly acidic loamy soils or slightly acidic base-rich soils. The granites are overlain by the same acid loamy soils, along with very acid loamy upland soils with a wet peaty surface, very acid upland soils with a peaty surface, and on Bodmin Moor and Dartmoor blanket bog peat soils. Extensive areas on the St Austell Granite are restored soils as a result of the china clay (kaolinite) mining in this area. The soils on the Lizard Complex comprise slightly acidic base-rich soils and wet acid loamy and clayey soils.

Materials and methods

Soil sampling

Prior to sampling, 35 rural locations throughout Devon and Cornwall with (a) different underlying bedrock geology but (b) similar land-use, were identified as suitable for sampling based on examination of topographic maps, British Geological Survey geological maps and Google Earth imagery. Soil sampling was carried out between the 24th February and the 7th March 2016. Wherever possible, areas of managed grassland, ploughed and re-seeded for grazing, were selected for sampling. Sampling sites within these areas were selected away from sources of apparent introduced geological materials such as tracks and roadways. Localised areas of historic mining activity are widespread in SW England; however, these were also deliberately avoided as mineral contamination introduced into the surface environment near these sites is highly distinctive, and therefore not representative of the underlying bedrock-soil relationship (Pirrie et al., 2003). In the context of geolocation, identification of these distinctive mineral species would allow an unknown area to be identified with high precision; however, these signatures do not have wider relevance in localities without a significant history of mining contamination.

At each sampling location a 250 m long, linear transect was established. In some cases, transects were offset to take into account the orientation of field boundaries. Five samples were collected in total along the line of the transect, with the first sample at the start (0 m), followed by samples taken at distances of 10 m, 50 m, 100 m and 250 m along the transect. Sampling location co-ordinates were recorded using a handheld GPS.

To extract the soil sample, a labelled 35 mm diameter clean plastic sampling pot was pushed approximately 2 cm into the ground surface (Fig. 2). The edges of the pots are thin and effectively cut a clean edge into the soil profile. If possible, areas of exposed soil were preferentially selected for sampling. The *in-situ* sampling pots were digitally photographed, removed and then sealed with tamper evident lids and placed within zip lock plastic bags. The pots were then opened so that the exposed visible surface represents the lowest part of the sampled soil, estimated to be at a depth of between 1 and 2 cm below the surface. A subsample was removed from this lower surface and dried for 2 hours at a temperature of 50°C, before being sealed within a zip-lock plastic bag. In total, 175 soil samples were collected, subsampled and dried.

Mineral analysis

The initial (0 m) sample from each of the 35 locations was selected for mineral analysis (Table 2). In addition, one sampling location was selected at random (location 24, Porthtowan Formation metamorphosed mudstone) and all 5 samples collected from that location were also prepared for analysis.

Each soil subsample was gently disaggregated, placed into a 30 mm mould and mixed with epofix resin. The samples were allowed to cure for 24 hrs, labelled and back-filled with araldite resin and heated at 50°C for 2 hours. The blocks were then polished and carbon coated prior to mineral analysis. Mineral analysis of the 40 samples was carried out using automated scanning electron microscopy (SEM) with linked energy dispersive X-ray (EDX) spectrometers, based on QEMSCAN technology.

Automated SEM-EDS is a widely used method for mineral analysis (Armitage et al., 2010; Williamson et al., 2013; Eby et al., 2015) and has previously been used for the forensic analysis of soil samples (Pirrie and Rollinson, 2011; Pirrie et al., 2004, 2013, 2014). In brief, individual particles are located on the cut face of the polished block and are then phase mapped in cross section by the acquisition of energy dispersive X-ray spectra (in this study using 1000 counts/pixel) at a regular, operator defined spacing across the sample. The 1000 count spectra places limits of detection for elements present within the individual mineral grain at an abundance of approximately 3 atom percent (Andersen et al., 2009). In this study spectra were acquired across the sample using a 6 µm spacing, and the particle size range accepted for analysis was 9 µm to 800 µm. Each measured spectrum is assigned to a mineral name or chemical grouping by matching the elemental signature against a user-defined classification scheme (Pirrie and Rollinson, 2011). The mineral categories used in this study are provided in Table 3.

In each soil sample, >5000 individual mineral grains were analysed, based on the acquisition of between 50,734 and 487,685 EDS analysis points per sample. The number of EDS analyses is controlled by the size of the individual soil particles, such that finer-grained particles are effectively mapped by a smaller number of spectra than a larger particle (Table 2). Each sample took between 20 and 60 minutes to be analysed, showing that the methodology is sufficient for rapid sample screening. The automated mineralogy data were acquired using an FEI 650F scanning electron microscope, with an accelerating voltage of 25kv, equipped with twin Bruker 30 mm^2 Quantax spectrometers, and the data were processed using iDiscover 5.3 software. The data outputs derived from the automated mineral analysis used in this study are: modal mineralogy, mean mineral particle size and QEMSCAN mineral and phase composition particle maps.

Results

In the following description the mineral abundance is referred to as major >10%, minor 1-10% and trace <1% abundance in the measured sample.

Soil mineralogy variation

The variation in the modal mineralogy for the 35 different sampling locations across SW England is shown in Figs. 3a – f, and tabulated in Table 4. Although there is a range in bedrock geology in the study area the majority of the soil samples analysed are dominated by the same principal mineral types: quartz, plagioclase, K-feldspar, muscovite, biotite, chlorite, kaolinite, Fe silicates, Mg silicates, hornblende and tourmaline (Fig. 3a, c and e, Table 4). Less abundant minerals present are: epidote group minerals, sillimanite, topaz, other silicates, calcite, rutile, ilmenite, Fe-Mn oxides, chromite, apatite, zircon, xenotime, Ce phosphates, Fe/Cu sulphides, gypsum and “others” (Fig. 3b, d, and f, Table 4). However, although the same major/minor and trace minerals tend to co-occur throughout the samples analysed, their relative abundance varies considerably (Fig. 3a). When the data are combined by the location rock type as described in Table 1, differences both between and within these groups are observed. Although there is some mineralogical variation within each lithological group, there is greater variation in modal mineralogy between the different lithological groupings than observed within an individual group. These differences between lithological groups indicate the potential for the ‘type’ of geology to be identified in an unknown sample. The observed difference detected between samples of the same lithology highlights that, within the study area, there is potential for individual locations to be identified by their particular signatures.

In addition to the modal mineralogical dataset, QEMSCAN particle compositional images provide further means of classifying differences between the analysed soils. These reveal textural relationships between different mineral phases in the samples relating to grain size and mineral association, which can vary depending on the bedrock lithology on which the soil was developed. Representative particle images for selected soil samples developed on the different bedrock groups are shown in Fig. 4. Clear differences are observed in the mineral textures for soils developed on different rock types. For example, soils underlain by granitic bedrock include coarse grains of quartz, feldspar and mica minerals, whereas soil particles derived from metasedimentary rocks are highly heterogeneous, principally comprising grains of quartz intermixed with fine-grained clay minerals. No two soil samples analysed contain the same mineral types with the same relative abundance, grain size and texture, reflecting the distinctive nature of soil composition at different locations. The differences in characteristics between soils developed on different underlying bedrock, which are evident in groupings of automated mineralogy data (Fig. 3), could allow broad areas to be identified or ruled out by identifying the likely source lithologies from an unknown sample.

Soils grouped by bedrock lithology

To assess the mineralogical variation throughout the study area in more detail the data for the same, or similar, bedrock geology is compared. Identification of differences in soil mineralogy between samples arising from similar bedrock geologies is required to define the range of compositions which could be indicative of a particular lithology. If specific differences are present, these could also be used to further refine the spatial scale of a geolocation assessment, such as identifying a particular group out of several candidate units within a region.

Granites. Six soil samples developed upon granite bedrock were analysed. These soils were identified as being derived from an underlying granitic geology by the consistent abundance of large (~100 µm) grains of quartz, plagioclase, K feldspar, biotite and muscovite (e.g. Fig. 4). The Cornubian granites have been subdivided into five mineralogical types and individual named intrusions are commonly composite with more than one granite type present (Simons et al., 2016). Each of the soils sampled had distinctive compositions in minor and trace mineralogy, which were consistent with at least one of the characteristics of the underlying subcrop. This is indicative of the known spatial heterogeneity of the individual granite bodies (Simons et al., 2016).

Key mineralogical parameters and the known underlying granite types are presented in Table 5. The relative abundance of biotite and muscovite was indicative of biotite granite (G3, biotite > muscovite) underlying the Lands End granite soil, and two-mica granite (G1, biotite ≈ muscovite) underlying the Tregonning-Godolphin and Carnmenellis Granite soils. High relative abundance of tourmaline in the St Austell and Dartmoor samples was indicative of G4 tourmaline granites in these sample areas. The Bodmin Moor Granite was characterised by an increased abundance of muscovite relative to biotite, consistent with muscovite granite (G2), and the abundance of ‘topaz’ and ‘sillimanite’ (suggestive of the accessory mineral andalusite (Simons et al., 2016), which would be grouped with sillimanite during QEMSCAN analysis) was distinctive in this sample. Other mineralogical signatures in the group included kaolinite abundance, which was particularly high in the St Austell Granite soil. Replacement of feldspar by kaolinite is present in all of the granites of SW England, however, the St Austell Granite exhibits the most extensive kaolinisation (Ellis and Scott, 2004), and the high abundance in this sample is evidence that this mineralogical signature is preserved in the soil.

Within the study area, soils developed on granites possess both common overall characteristics that allows the underlying lithology to be identified, but also sufficient variety between samples to permit individual subcrops to be distinguished. Links between the composition of a soil and published characterisation of the granite type (Ellis and Scott, 2004; Simons et al., 2016) were possible, such that key mineral signatures can be used to rule out one or more of the subcrops as an unlikely source of the soil. This approach is powerful, but may be highly limited to locations or rock types which display this degree of mineralogical variation.

Mafic igneous rock. Six soil samples were analysed from locations where the reported bedrock geology was gabbro, dolerite or basalt (Table 3), and were grouped together as 'mafic igneous' rock types. Modal mineralogy data (Fig 3a and 2b) shows that although there is some variation between these samples, they form a consistent grouping characterised by high abundance of chlorite and the presence of Mg silicates, both of which are indicative of altered mafic minerals.

Soils developed on dolerites and gabbros had similar overall composition and texture (e.g. Fig 4), comprising several species of coarse mono-minerallic grains suggestive of an igneous basement rock. The samples are however, subtly different to each other, with the gabbro derived soils containing more abundant K feldspar, hornblende and kaolinite, and less abundant Mg silicates, chlorite and Fe silicates than the dolerites. Highly specific mineral signatures were detected in some samples, in particular the presence of abundant hornblende in Sample 15, which within the study area was distinctive of the Trelan and Crousa Gabbro, part of the Lizard Complex.

The two soil samples from locations underlain by either basaltic calcareous tuffs of the Tintagel Volcanic Formation or the basalts-mudstones of the Milton Abbott Formation were distinct from the soils derived from dolerite/gabbro bedrock. In general, the soils associated with basaltic lithologies contain less abundant plagioclase, hornblende and tourmaline and more abundant K feldspar and biotite, although it should be noted that the basaltic lithologies are interbedded with mudstones. In addition, whilst the Tintagel Volcanic Formation is described as comprising calcareous basaltic tuffs, very few (0.10%) grains in the soil sample derived from this unit reported to the calcite mineral grouping. Geochemical and mineralogical studies have indicated that the Tintagel Volcanic Formation comprises both calcite-rich but also calcite-poor lithologies (Rice-Birchall and Floyd, 1988), hence it is possible that the sample collected was from soils developed on a calcite-poor lithological unit.

The soils underlain by mafic-igneous lithologies were found to form a consistent grouping of modal mineralogy and texture. Owing to the range of rock types grouped together, aspects of the mineralogy of both individual samples and rock types (e.g. gabbro vs dolerite) were found to be distinctive.

In contrast to granitic derived soils, the mineralogy of these samples is more strongly controlled by alteration products of mafic minerals, rather than the persistence of lithic fragments.

Metamorphic rocks of the Lizard Complex. Four soil samples collected from locations underlain by metamorphic rocks were analysed, all associated with the Lizard Complex (Fig. 1). It should be noted that this grouping of soil samples is rather arbitrary, as it does not necessarily represent a homogenous compositional grouping but could include rocks of differing mineralogy depending on protolith composition and metamorphic grade. Some of the samples showed similar major mineralogy to locations within the mafic-igneous group, however, they were identified as metamorphic derived soils by the enhanced abundance of mineral groups such as hornblende, epidote and Mg-silicates and a lower abundance of rutile and ilmenite.

Trends relating to specific units within the Lizard Complex were identified. Soil sample 14 has the highest abundance of hornblende (12.8%) and epidote (1.6%) of the entire sample set. Within the sample area this combination of hornblende and epidote, a common greenschist-facies metamorphic mineral, is distinctive of the Traboe Hornblende Schist underlying this sample location.

The abundance of Mg-silicate minerals was expected to be a distinguishing characteristic of soils underlain by the Lizard Serpentinite, as this is the compositional grouping which includes serpentine-group minerals (Table 3). However, although the soil from this area (Sample 16) contained 1.4% Mg-silicates (serpentine group minerals), two samples from other areas contained higher abundances; samples 4 (11.1% Mg-silicates, gneiss) and 12 (3.9% Mg-silicates, dolerite). The published geological map indicated that sampling location 4 was underlain by the Kennack Gneiss. However, this lithology has a patchy / localised distribution with pods of granitic gneiss surrounded by serpentinite. Consequently, the soil mineralogy data may be interpreted to suggest that either: (a) the published map is incorrect, and that the bedrock geology at this location is actually serpentinite, or that (b) periglacial processes have introduced serpentinite derived surficial deposits at this location. It should however, also be noted that both the Kennack Gneiss

(Sample 4) and Nare Head Dolerite (Sample 12) contain amphibole group minerals (Barnes et al., 1979), which (other than hornblende) would be characterised under the Mg silicate QEMSCAN grouping. Within the study area, soils with abundant Mg-silicate (>1%) were consistent with several underlying lithologies, however, this was highly distinctive, relating to three out of the thirty five locations sampled. More generally, this finding demonstrates the importance of obtaining detailed information on the composition of candidate lithologies to check for consistency with observed soil mineralogy.

Reference to regional soil geochemistry surveys revealed that a characteristic feature of the soils present on the Lizard Complex is a high relative abundance of chromium (Cr) (BGS, 2015). This was supported in the modal mineralogy data with elevated abundances of the mineral chrome spinel (Table 2) for soils developed on the Lizard Serpentinite (Sample 16) and also at sample location 4. The abundance of chrome spinel along with the serpentine minerals would support the interpretation that sampling location 4 is not underlain by the Kennack Gneiss as indicated by the published map, but instead is underlain by serpentinite. This therefore provides a highly location specific signature which is absent in soils developed on chromium-poor rocks elsewhere in the sample region.

Metamorphosed mudstone. The dominant geological unit throughout the study area is Devonian low-grade metamorphosed mudstones and sandstones, the original deposition of which was strongly controlled by tectonics, within a series of separate depositional basins in the study area; Gramscatho, Looe, South Devon and Tavy (Fig. 1) (Leveridge, 2011; Leveridge and Shail, 2011b).

Thirteen soil samples developed upon Devonian metamorphosed mudstones were analysed, covering each of the depositional basins (Fig. 3c, d). These samples had a characteristic fine-grained texture (Fig. 4) and similar modal mineralogy, being dominated by major quartz, K feldspar, muscovite, biotite and chlorite along with minor/trace plagioclase, kaolinite and tourmaline. This combination of features permitted distinction of these samples as being derived from a metasedimentary source.

Despite the similar overall characteristics, it is clear that there are mineralogical variations within the dataset related to depositional basin (Fig. 3c, d). For example, soil samples collected from locations up to ~60 km apart across the South Devon Basin (19, 23, 28 and 29) are all quartz-poor (less than 20% quartz, Fig. 3c), whilst those collected from the Gramscatho Basin (13, 18, 24, 26), again up to 60 km apart, have a consistently higher quartz abundance (>20-30%). The changing relative abundance of quartz may reflect differences in soil particle size, as quartz typically comprises larger sand/silt sized particles. However, the average particle size for Gramscatho Basin samples was finer than in the South Devon Basin samples, and therefore the quartz variations are likely to be representative of mineralogical differences between the locations rather than particle size.

In the soil mineralogy data, samples collected from the Trevose Slate (Sample 19, Devon Basin) and the Tredorn Slate (Sample 21, Tavy Basin) formations both have elevated levels of chrome spinel (Table 2). Although this is not described in regional scale geological mapping, published soil geochemical surveys show an elevated chromium anomaly in these regions (BGS, 2015) consistent with the measured mineralogical data. Whilst Cr-rich soils are observed in other regions of the study area such as the Lizard Complex, a soil with meta-mudstone characteristics and the presence of Cr-spinel as a minor mineral indicates a restricted provenance to the Trevose-Tredorn formations.

Metamorphosed sandstone-mudstone. Three soil samples were analysed from locations underlain by either metamorphosed Devonian sandstones or interbedded sandstones / mudstones (Figs. 3e and f). These were differentiated from the metamorphosed Devonian mudstones principally by texture; soils developed on lithologies with a sandstone component contained quartz as both sand-silt grade monominerallic and sand-grade polyminerallic grains (Fig. 5). The abundance of quartz is another key differentiator. Sample 9, which was taken from a sandstone bedrock location has very high quartz abundance (73.7%), whilst soils from interbedded locations (samples 11 and 25) are intermediate in quartz abundance between sandstone and mudstone locations. In these cases, the higher abundance of quartz is indicative of the coarser grain size of the underlying rock at these locations, which along with grain texture, may allow the identification of soils developed on different grain size sedimentary or metasedimentary rocks.

Carboniferous sedimentary rocks. Sedimentary rocks of Carboniferous age which have undergone Variscan deformation and very low grade regional metamorphism occur within the eastern part of the study area. Three soil samples developed on Carboniferous mudstones, interbedded mudstones and sandstones, and chert were analysed (Fig. 3e and f). Soils developed on locations underlain by Carboniferous mudstone and chert formations (Samples 30 and 31) had similar fine-grained textures to the Devonian metamorphosed mudstone samples (e.g. Fig. 4 d and f). However, the lower metamorphic grade of the Carboniferous rock resulted in mineralogical differences, with lower biotite and muscovite (illite) abundances and more abundant chlorite, plagioclase and quartz reflecting lower thermal maturity of these bedrocks. The abundance of quartz in the 'chert' sample was not as high as may be expected, and therefore may arise from another interbedded component (e.g. mudstone) of the heterogeneous Teign (Newton) Chert Formation.

The sandstone-mudstone nature of Sample 33 could be readily identified amongst the Carboniferous sedimentary samples by the high abundance of quartz and coarse grain size. However, it could not be readily distinguished from the Devonian metamorphosed location (Sample 9); unlike the mudstones, little mineralogical change would be expected during the low grade metamorphism of a quartz-rich sandstone and therefore no difference between these samples was detected. This finding highlights that using automated mineralogy alone it may be difficult to distinguish between lower grade metamorphosed sediments and 'pure' sedimentary lithologies, and in areas predominantly composed of such rocks a wider suite of techniques will be required.

Variation within a single location

To examine the spatial variation at a more local scale in detail, one sample was selected at random and all five sampling points along a 0 to 250 m transect were prepared for analysis. The modal mineralogy for these five samples, along with the replicate sample analysed from the first sampling point are illustrated in Fig. 6 and the data are presented in Table 6. The mineralogical data show the closest correspondence between the two replicate samples, but the overall suite of five samples collected over a distance of 250 m within the same agricultural field are a closely comparable data set. The data for the five samples along the individual transect show lower variance than the samples analysed from the different sampling locations. Thus if the data for the 35 separate sampling locations across the region are compared with the data for these samples, then it is clear that the soil modal mineralogical data would allow the identification of the correct sampling location. This supports the modal mineralogy data from the whole sample suite, which indicates that within the study area, the underlying bedrock geology is the dominant control on soil mineral composition.

Discussion

For forensic geolocation based on a soil sample, the ideal scenario would be to have access to representative samples from all the regions of interest to allow comparisons to be drawn directly. However, this is often not practical, and may be impossible in wide-area search investigations, which would be characteristic in nuclear forensics. Therefore, it is necessary to rely on comparison of measurable properties of an unknown soil with reference datasets to establish the potential provenance of a sample.

Most spatial soil surveys typically describe parameters such as grain size, organic content, pH, colour etc, which for geolocation purposes are not sufficiently descriptive. For example, soil surveys from the study area show little variation other than the major contrasts between upland peat soils versus the predominantly managed arable and grazing land. This contrasts markedly with the clear differences in soil mineralogy and particle textures revealed by automated mineralogical analysis, and this variety indicates that, within the studied area, soil mineralogy is a more distinctive indicator of location than the overall soil classification or texture.

There are few comprehensive global datasets for soil mineralogy. The United States Geological Survey has an open access database for soil mineralogy of the USA, comprising 4857 samples, which equates to a sampling density of 1 sample per 1600 km^2 (Smith et al., 2014). As such this shows regional trends, but is of less value for forensic investigations. In the absence of comprehensive datasets for detailed soil mineralogy, other reference datasets must be used to predict locations at which a particular soil mineralogy may be found. In this paper we have demonstrated that, for the study area, soil mineralogy is consistent with the local underlying geology as represented by widely available regional scale geological mapping. Local scale geochemical surveys (BGS, 2015) can add an extra level of detail, such as the highly localised distribution of chromium around the Trevose and Tredorn Slate formation locations, which was detected as a high relative abundance of chrome-spinel in these soils samples.

The nature of the correlation between bedrock composition and soil mineralogy will depend on a number of factors specific to the study area. In localities dominated by physical weathering, with typically arid to semi-arid climates, soils are more likely to be composed of liberated relic minerals grain and lithological fragments, and it is expected that there will be a strong correlation between the mineralogical composition of soils and the near-surface geology. However, in areas where chemical weathering predominates, and/or where soil profiles relate to past intervals of geological weathering, soil mineralogy may be substantially altered from the parent rock. Owing to the oceanic climate, soil formation in the study area is dominated by chemical weathering and hence is more representative of the second condition.

Soil mineralogy was also sufficient to distinguish individual occurrences of most of the lithology types within the study area. Consideration of the minor phases present in the granites showed differences related to the specific granite type whereas the mineralogy of metasediment samples was shown to differ across different depositional basins. The extent to which this might be used to determine a specific location, rather than just distinguish two dissimilar samples, was varied and depended on the mineralogical variety within the parent rock. It was only in the case of the sandstone samples 9 and 33 that these distinctions could not be made; including between different metamorphosed grades of this lithology. Nevertheless, these results highlight the potential of a two-stage approach to predictive geolocation, whereby a generic lithology may be identified in the first instance, and, in favourable locations, further refinement made by considering the details of local variations in specific occurrences of that lithology. Whilst regional scale mapping is probably sufficient for the first aspect, more detailed data sources, such as specific publications, may be required for the second.

In the context of nuclear forensics, the capability provided by soil analysis to identify even the generic geological background may be of particular value. In many cases, such data may permit some potential locations to be excluded, rather than indicating an individual specific target location. The significance of this is that during a nuclear forensic investigation, the nature of a material being examined may indicate that it could only have been derived from a limited number of potential installations. Consideration of geolocation evidence (where present) may therefore allow some of these candidate sources to be ruled out based on their environmental setting, substantially narrowing the scope of the investigation. Further work to consider the collection and analysis of this type of evidence in nuclear forensic scenarios is needed. Although it may not be expected to recover soil traces in all cases, the power of this analysis to distinguish locations, if soil is present, highlights its value to these complex investigations.

Conclusions

In this study we aimed to test the extent to which soil mineralogy can be used to predict an underlying geological rock type, and how distinctive this may be of an individual unit of that lithology. The study area in SW England may represent a ‘worst-case’ type environment for this technique, as soils in the area are highly chemically altered from the host rock mineralogy through chemical weathering and human activity. The repetition of many of the major rock types throughout the area also challenged the capability of this analysis to distinguish different locations with similar underlying rock types. In all sampled locations, signatures of the underlying bedrock geology were detected in the soil mineralogy and particle textures, and in 33 out of the 35 samples, location-specific were detected permitting different units of the same major rock type to be distinguished.

This type of analysis is a powerful method for the identification of potential underlying bedrock units from soil samples, which can be used with readily available regional scale geological mapping to identify, and just as importantly rule out, candidate regions based on the known geology. The importance of this information will depend on the extent of geological variation within the area of investigation; if the entire area is underlain by the same lithology then other geolocation indicators may be more valuable.

In our area of interest in nuclear forensics, the provenance of a found nuclear material may be already somewhat constrained by known holdings and operations, and therefore identification of the geology type may allow some potential sources to be ruled out. Challenges relating to transfer and collection of soil evidence in these scenarios must be evaluated, however, consideration of environmental signatures such as soil evidence has the potential to provide a unique insight and perspective in these complex investigations.

Acknowledgements

We thank Holly Campbell (Helford Geoscience LLP) for assistance with the soil sampling and preparation of samples for analysis. Figure 1B reproduced from R.K. Shail and B.E. Leveridge. The Rhenohercynian passive margin of SW England: Development, inversion and extensional reactivation. Comptes Rendus Geoscience, 2009, 341 (issue2-3), 140-155. Copyright (c) 2009 published by Elsevier Masson SAS. All rights reserved. Funding for this programme of research was provided by AWE plc to Helford Geoscience LLP.

References

Anderson, J.C.O., Rollinson, G.K., Snook, B., Herrington, R. & Fairhurst, R.J. 2009. Use of QEMSCAN for the characterisation of Ni-rich and Ni-poor goethite in laterite ores. *Minerals Engineering*, **22**, 1119-1129.

Armitage, P.J., Worden, R.H., Faulkner, D.R., Aplin, A.C., Butcher, A.R. & Iliffe, J. 2010. Diagenetic and sedimentary controls on porosity in Lower Carboniferous fine-grained lithologies, Krechba field, Algeria: A petrological study of a caprock to a carbon capture site. *Marine and Petroleum Geology*, **27**, 1395-1410.

Barnes, R.P., Andrews, J.R. & Badham, J.P.N. 1979. Preliminary investigations of South Cornish melanges. *Proceedings of the Ussher Society*, **4(3)**, 262-268.

Beamish, D. 2015. Relationships between gamma-ray attenuation and soils in SW England. *Geoderma*, **259-260**, 174-186.

Benham, A.J., McEvoy, F.M. & Rollin, K.E. 2005. Potential for stratiform massive sulphide mineralisation in south-west England. *Transactions of the Institute of Mining and Metallurgy, Section B,* **113**, 227-246.

British Geological Survey, NERC. 2015. Geochemical baseline survey of the environment, South West England.

Bowen, A.M. & Caven, E.A. 2013. Forensic provenance investigations of soil and sediment samples. *In*: Pirrie, D., Ruffell, A. & Dawson, L.A. (eds) *Environmental and Criminal Geoforensics*. Geological Society, London, Special Publication, 384, 9-25.

Bull, P.A., Parker, A. & Morgan, R.M. 2006. The forensic analysis of soils and sediment taken from the cast of a footprint. *Forensic Science International*, **162**, 6–12.

Caritat, P., Simpson, T. & Woods, B. 2019. Predictive soil provenancing (PSP): an innovative forensic soil provenance analysis tool. *Journal of Forensic Sciences*. doi: 10.1111/1556-4029.14060.

Cranfield Soil and Agrifood Institute, soilscapes database, last accessed 21/09/2016, http://www.landis.org.uk/soilscapes.

Eby, G.N., Chamley, N., Pirrie, D., Hermes, R., Smoglia, J. & Rollinson, G. 2015. Trinitite redux: Mineralogy and petrology. *American Mineralogist*, **100**, 427-441.

Edwards, R.A., Warrington, G., Scrivener, R.C., Jones, N.S., Haslam, H.W., Ault, L. 1997. The Exeter Group, south Devon, England: a contribution to the early post-Variscan stratigraphy of northwest Europe. *Geological Magazine*, **134**, 177-197.

Ellis, R.J. & Scott, P.W. 2004. Evaluation of hyperspectral remote sensing as a means of environmental monitoring in the St. Austell china clay (kaolin) region, Cornwall, UK. *Remote Sensing of the Environment*, **93**, 118-130.

Fitzpatrick, R., Raven, M.D. & Forrester, S.T. 2009. A systematic approach to soil forensics: Criminal case studies involving transference from crime scene to forensic evidence. *In*: Ritz, K., Dawson, L. & Miller, D. (eds), *Criminal and Environmental Soil Forensics*. Springer, 105-127.

Harrison, S., Anderson, E. & Passmore, D.G. 1998. A small glacial cirque basin on Exmoor, Somerset. *Proceedings of the Geologists Association*, **109**, 149-158.

Keegan, E., Kristo, M.J., Toole, K., Kips, R. & Young, E. 2016. Nuclear Forensics: Scientific Analysis Supporting Law Enforcement and Nuclear Security Investigations. *Analytical Chemistry*, **88**, 1496-1505.

Kirkwood, C., Everett, P., Ferreira, A. & Lister, B. 2016. Stream sediment geochemistry as a tool for enhancing geological understanding: An overview of new data from south west England. *Journal of Geochemical Exploration*, **163**, 28-40.

Kosanic, A., Harrison, S. Anderson, K. & Kavcic, I. 2014. Present and historical climate variability in South West England. *Climate Change*, **124**, 221-237.

Lark, R.M. & Rawlins, B.G. 2008. Can we predict the provenance of a soil sample for forensic purposes by reference to a spatial database? *European Journal of Soil Science*, **59**, 1000-1006.

Leveridge, B.E. 2011. The Looe, South Devon and Tavy basins: the Devonian rifted passive margin successions. *Proceedings of the Geologists Association*, **122**, 616–717.

Leveridge, B.E. & Shail, R.K. 2011a. The Gramscatho Basin, south Cornwall, UK: Devonian active margin successions. *Proceedings of the Geologists Association*, **122**, 568–615.

Leveridge, B.E. & Shail, R.K. 2011b. The marine Devonian stratigraphy of GB. *Proceedings of the Geologists Association*, **122**, 540-567.

Mayer, K., Wallenius, M. & Varga, Z. 2012. Nuclear forensic science: Correlating measureable material parameters to the history of nuclear material. *Chemical Reviews*, **13**, 884 - 900.

Mayer, K., Wallenius, M., Lützenkirchen, K., Horta, J., Nicholl, A., Rasmussen, G., van Belle, P., Varga, Z., Buda, R., Erdmann, N., Kratz, J.-V., Trautmann, N., Fifield, K., Tims, S., Fröhlich, M. & Steier, P. 2015. Uranium from German Nuclear Power Projects of the 1940s – A Nuclear Forensic Investigation. *Angewandte Chemie, International Edition*, **54**, 13137.

Owens, P.N., Blake, W.H., Gaspar, L., Gateuille, D., Koiter, A.J., Lobb, D.A., Petticrew, E.L., Reiffarth, D.G., Smith, H.G. & Woodward, J.C. 2016. Fingerprinting and tracing the source of soils and sediments: Earth and ocean science, geoarchaeological, forensic and human health implications. *Earth Science Reviews*, **162**, 1-23.

Pirrie, D & Rollinson, G.K. 2011. Unlocking the application of automated mineralogy. *Geology Today*, **27**, 226-235.

Pirrie, D. & Ruffell, A. 2012. Soils and geological trace evidence. *In*: Marquez Grant, N. and Roberts, J. (eds) *Forensic Ecology Handbook*. Blackwell-Wiley, 183-201.

Pirrie, D. & Shail, R.K. 2018. Mud and metal; the impact of historical mining on the estuaries of SW England, UK. *Geology Today*, **34**, 215-223.

Pirrie, D., Power, M.R., Rollinson, G., Camm, G.S., Hughes, S.H., Butcher, A.R. & Hughes, P. 2003. The spatial distribution and source of arsenic, copper, tin and zinc within the surface sediments of the Fal Estuary, Cornwall, UK. *Sedimentology*, **50**, 579-595.

Pirrie, D., Butcher, A.R., Power, M.R., Gottlieb, P. & Miller, G.L. 2004. Rapid quantitative mineral and phase analysis using automated scanning electron microscopy (QemSCAN); potential applications in forensic geoscience. *In*: Pye, K. & Croft, D. (eds), *Forensic Geoscience*. Geological Society, London, Special Publication, 232, 123-136.

Pirrie, D., Rollinson, G.K., Power, M.R. & Webb, J. 2013. Automated forensic soil mineral analysis; testing the potential of lithotyping, *In*: Pirrie, D., Ruffell, A. & Dawson, L.A. (eds) *Environmental and criminal geoforensics*. Geological Society of London, Special Publication, 384, 47-64.

Pirrie, D., Rollinson, G.K., Andersen, J.A., Wootton, D. & Moorhead, S. 2014. Soil forensics as a tool to test reported artefact find sites. *Journal of Archaeological Science*, **41**, 461-473.

Pirrie, D., Dawson, L. & Graham, G. 2017. Predictive geolocation: forensic soil analysis for provenance determination. *Episodes*, **40**, 141-147.

Rice-Birchall, B. & Floyd, P.A. 1988. Geochemical and source characteristics of the Tintagel Volcanic Formation. *Proceedings of the Ussher Society*, **7**, 52-55.

Shail, R.K. & Leveridge, B.E. 2009. The Rhenohercynian passive margin of SW England: development, inversion and extensional reactivation. *Comptes Rendus Geoscience*, **341**, 140-155.

Simons, B., Pirrie, D., Rollinson, G.K. & Shail, R.K. 2011. Geochemical and mineralogical record of the impact of mining on the Teign estuary, Devon, UK. *Geoscience in South-West England*, **12**, 339-350.

Simons, B., Shail, R.K. & Andersen, J.C.O. 2016. The petrogenesis of the Early Permian Variscan granites of the Cornubian Batholith: Lower plate post-collisional peraluminous magmatism in the Rhenohercynian Zone of SW England. *Lithos*, **260**, 76-94.

Smith, D.B., Cannon, W.F., Woodruff, L.G., Solano, Federico & Ellefsen, K.J., 2014. Geochemical and mineralogical maps for soils of the conterminous United States. *U.S. Geological Survey Open-File Report*, 2014–1082, 386 p. https://dx.doi.org/10.3133/ofr20141082.

Stern, L.A., Webb, J.B., Willard, D.A., Bernhardt, C.E., Korejwo, D.A., Bottrell, M.C., McMahon, G.B., McMillan, N.J., Schuetter, J.M. & Hietpas, J. 2019. Geographic attribution of soils using probabilistic modeling of GIS data for forensic search efforts. *Geochemistry, Geophysics, Geosystems*, **20**, 1-20.

Wallenius M., Mayer, K. & Ray, I. 2006. Nuclear forensic investigations: Two case studies. *Forensic Science International*, **156**, 55-62.

Williamson, B.J., Rollinson, G. & Pirrie, D. 2013. Automated mineralogical analysis of PM^{10}: New parameters for assessing PM toxicity. *Environmental Science and Technology*, **47**, 5570-5577.

Figure captions

Fig. 1. Simplified maps showing distribution of sampling sites (A) and major near-surface geological features of SW England (B). Map B shows the main Devonian sedimentary basins (Gramscatho, Looe, South Devon and Tavy basins) along with the Lizard Ophiolite Complex (purple), the Start Complex and the exposed granites making up the Cornubian Batholith. Map A based on a Digimap extract © Crown Copyright and Database Right [June 2018]. Ordnance Survey (Digimap Licence). Map B from Shail and Leveridge (2009).

Fig. 2. Example images for soil sampling location 1, near Halwyn Farm, Mousehole, West Cornwall, underlain by the Lands End Granite. Five soil samples were collected from the managed grassland field (A) at sampling positions of 0 (1/1), 10 (1/2), 50 (1/3), 100 (1/4) and 250 m (1/5) along the transect (B). Soil samples were collected by inserting a clean, single use plastic vial into the soil to a depth of 1-2 cm (C). Map A based on a Digimap extract © Crown Copyright and Database Right [June 2018]. Ordnance Survey (Digimap Licence).

Fig. 3. Modal mineralogy of the soil samples collected throughout Cornwall and Devon, SW England, grouped by lithology according to Table 2. Charts A, C and E show relative abundance of major (>10%) and minor (1-10%) minerals, Charts B, D and F show relative abundance of minor (1-10%) and trace (<1%) minerals.

Fig. 4. Diagram showing the QEMSCAN false colour particle images for representative samples from the six major bedrock groups in SW England. (A) Sample 10/1 St Austell Granite, (B) Sample 12/1 Nare Head Dolerite, (C) Sample 14/1 Traboe Hornblende Schist (Traboe Cumulate Complex), Lizard Ophiolite Complex, (D) Sample 23/1 Devonian Polzeath Slate Formation metamorphosed mudstone, (E) Sample 9/1 Devonian Staddon Formation metamorphosed sandstone and (F) Sample 30/1 Carboniferous Teign (Newton) Chert Formation.

Fig. 5. Diagram showing the QEMSCAN false colour particle images for two soil samples developed on Devonian metasedimentary bedrock units from SW England. (A) Sample 9/1 Staddon Formation metamorphosed sandstones, (B) Sample 29/1 Tavy Formation metamorphosed mudstone. The quartz grain size and texture is a key discriminator of different sedimentary grades.

Fig. 6. Modal mineralogy of the 6 soil samples collected from sampling location 24 Porthtowan Formation bedrock, near Allet, Truro, Cornwall, along a 250 m transect. (A) Relative abundance of major (>10%) and minor (1-10%) minerals. (B) Relative abundance of minor (1-10%) and trace (<1%) minerals.

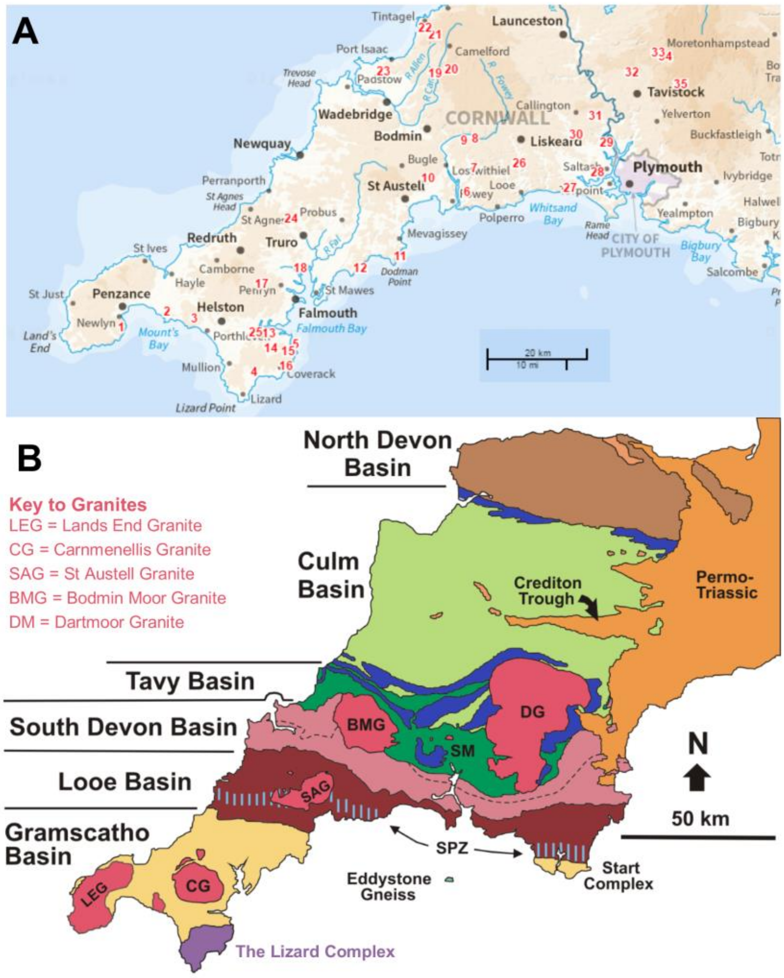
A
Tintagel
Launceston
Port Isaac
Camelford
Moretonhampstead
Trevose Head
Padstow
Tavistock
Wadebridge
Callington
Yelverton
CORNWALL
Bodmin
Liskeard
Buckfastleigh
Newquay
Bugle
Lostwithiel
Saltash
Plymouth
Perranporth
St Austell
Looe
Ivybridge
St Agnes Head
Probus
Polperro
Whitsand Bay
Yealmpton
Redruth
Truro
Mevagissey
Rame Head
CITY OF PLYMOUTH
Bigbury Bay
Bigbury
St Ives
Camborne
Dodman Point
Salcombe
Hayle
Penryn
St Mawes
St Just
Penzance
Helston
Falmouth
Newlyn
Falmouth Bay
Land's End
Mount's Bay
Mullion
Coverack
Lizard
Lizard Point
20 km
10 mi
B
North Devon Basin
Key to Granites
LEG = Lands End Granite
CG = Carnmenellis Granite
SAG = St Austell Granite
BMG = Bodmin Moor Granite
DM = Dartmoor Granite
Culm Basin
Crediton Trough
Permo-Triassic
Tavy Basin
South Devon Basin
BMG
DG
SM
N
Looe Basin
SAG
50 km
Gramscatho Basin
SPZ
Start Complex
Eddystone Gneiss
LEG
CG
The Lizard Complex

Figure 1.

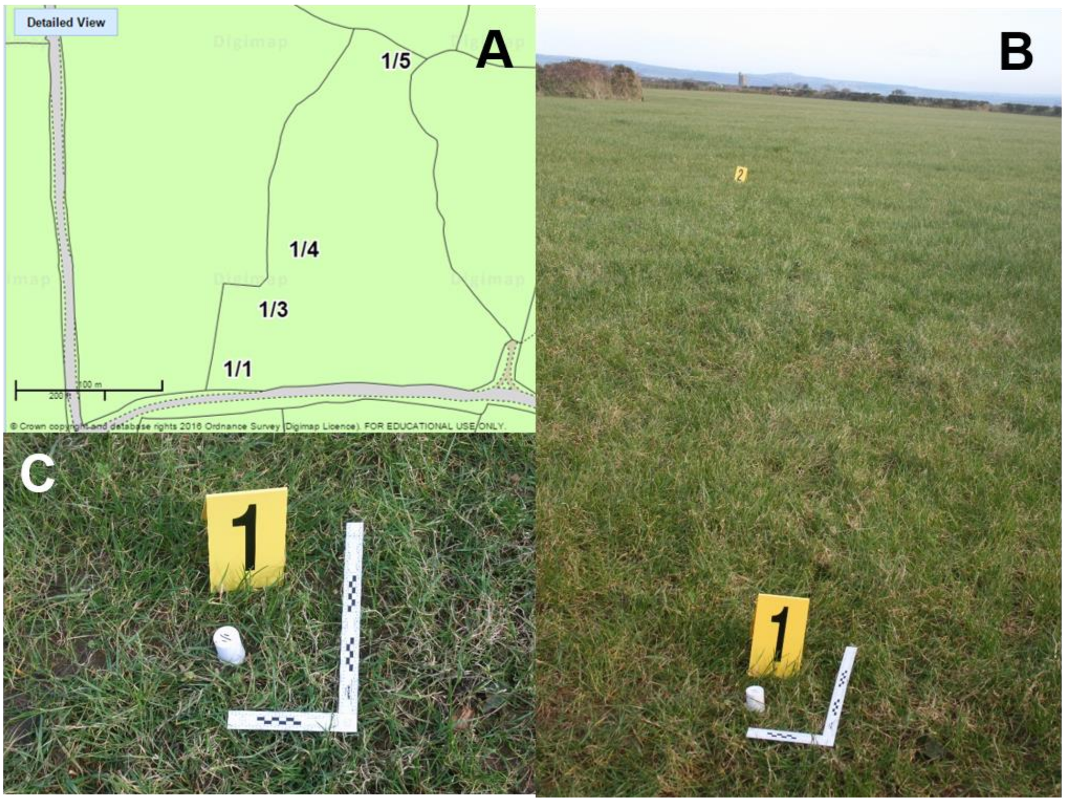

Figure. 2

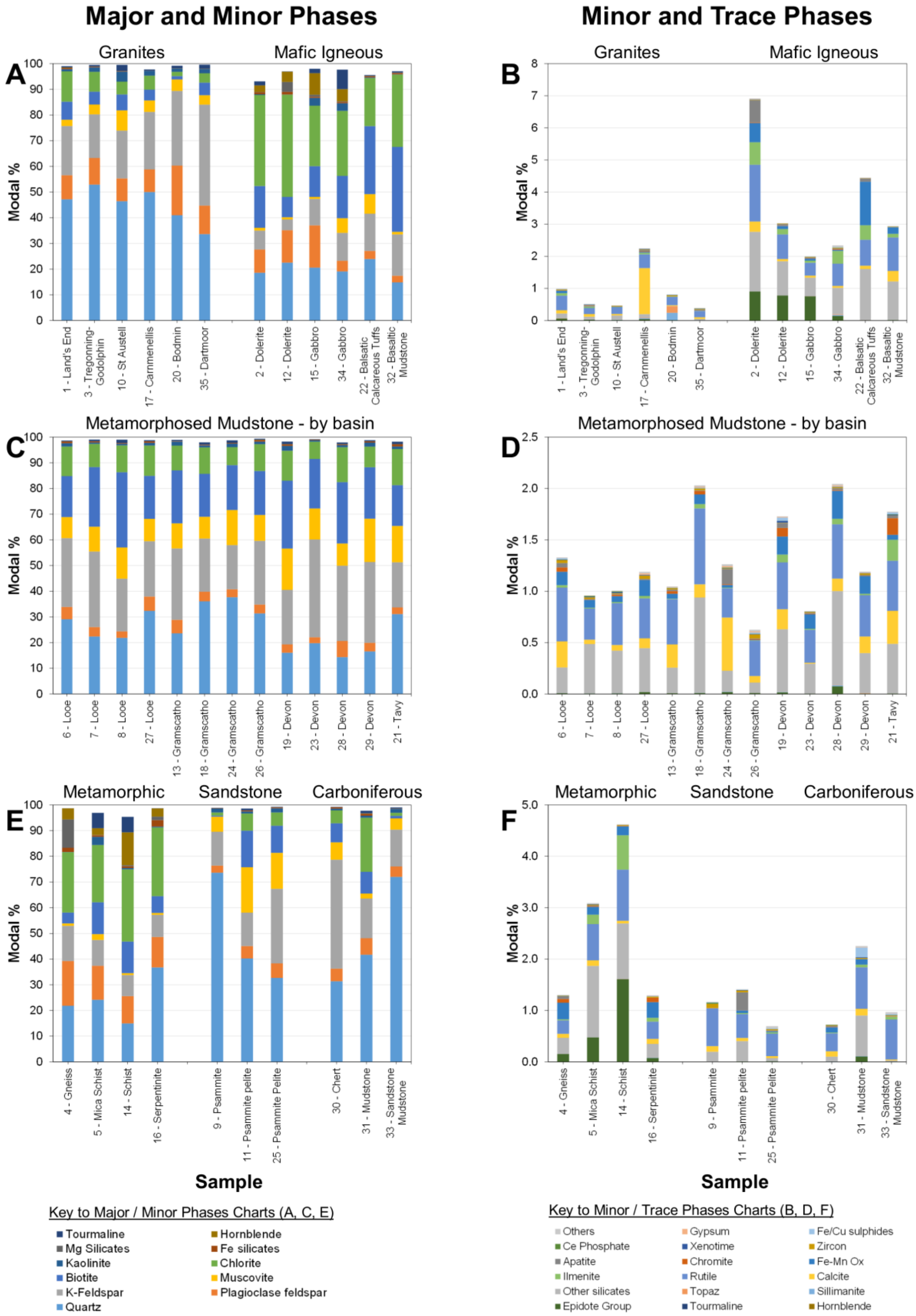
Major and Minor Phases
Minor and Trace Phases
A
B
C
D
E
F
Granites
Mafic Igneous
Metamorphosed Mudstone - by basin
Metamorphic
Sandstone
Carboniferous
Modal %
Sample
1 - Land's End
3 - Tregonning-Godolphin
10 - St Austell
17 - Carnmenellis
20 - Bodmin
35 - Dartmoor
2 - Dolerite
12 - Dolerite
15 - Gabbro
34 - Gabbro
22 - Balsatic Calcareous Tuffs
32 - Basaltic Mudstone
6 - Looe
7 - Looe
8 - Looe
27 - Looe
13 - Gramscatho
18 - Gramscatho
24 - Gramscatho
26 - Gramscatho
19 - Devon
23 - Devon
28 - Devon
29 - Devon
21 - Tavy
4 - Gneiss
5 - Mica Schist
14 - Schist
16 - Serpentinite
9 - Psammite
11 - Psammite pelite
25 - Psammite Pelite
30 - Chert
31 - Mudstone
33 - Sandstone Mudstone
Key to Major / Minor Phases Charts (A, C, E)
Tourmaline
Mg Silicates
Kaolinite
Biotite
K-Feldspar
Quartz
Hornblende
Fe silicates
Chlorite
Muscovite
Plagioclase feldspar
Key to Minor / Trace Phases Charts (B, D, F)
Others
Ce Phosphate
Apatite
Ilmenite
Other silicates
Epidote Group
Gypsum
Xenotime
Chromite
Rutile
Topaz
Tourmaline
Fe/Cu sulphides
Zircon
Fe-Mn Ox
Calcite
Sillimanite
Hornblende

Figure 3

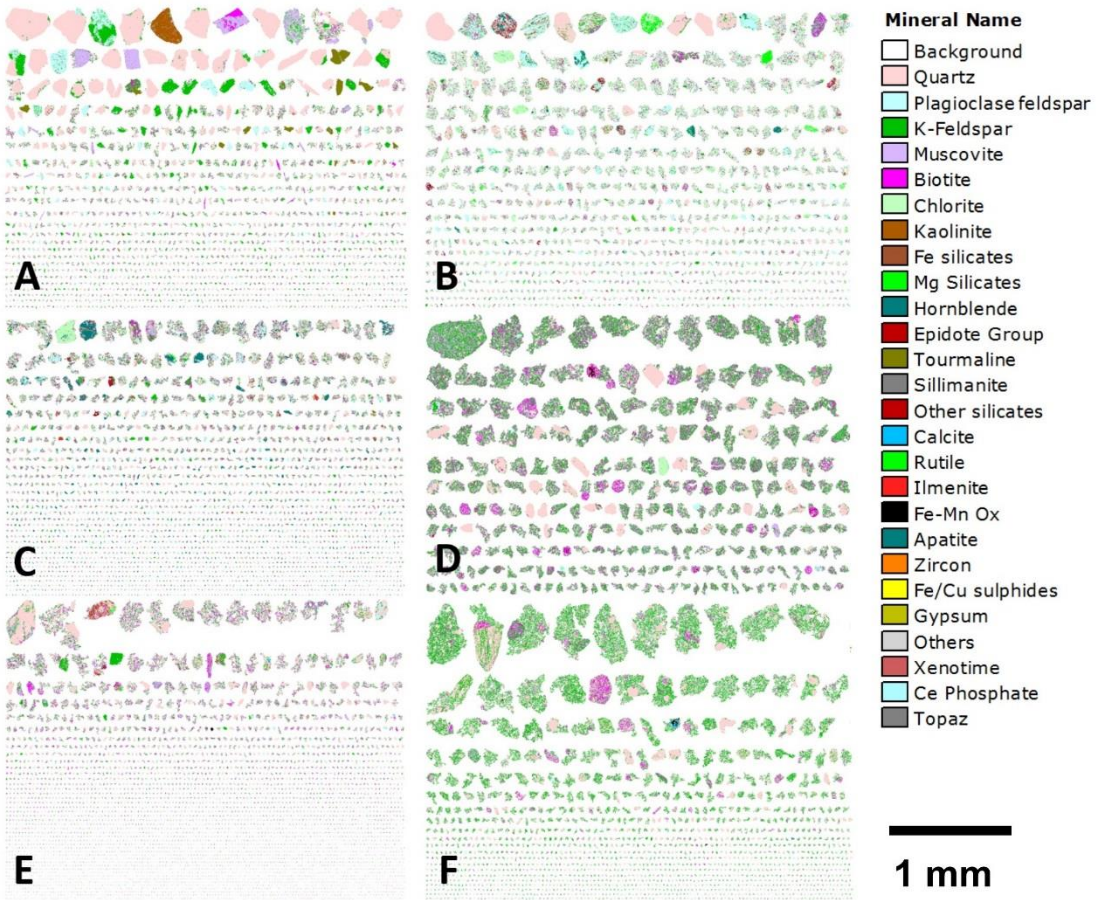
Mineral Name
Background
Quartz
Plagioclase feldspar
K-Feldspar
Muscovite
Biotite
Chlorite
Kaolinite
Fe silicates
Mg Silicates
Hornblende
Epidote Group
Tourmaline
Sillimanite
Other silicates
Calcite
Rutile
Ilmenite
Fe-Mn Ox
Apatite
Zircon
Fe/Cu sulphides
Gypsum
Others
Xenotime
Ce Phosphate
Topaz
A
B
C
D
E
F
1 mm

Figure 4.

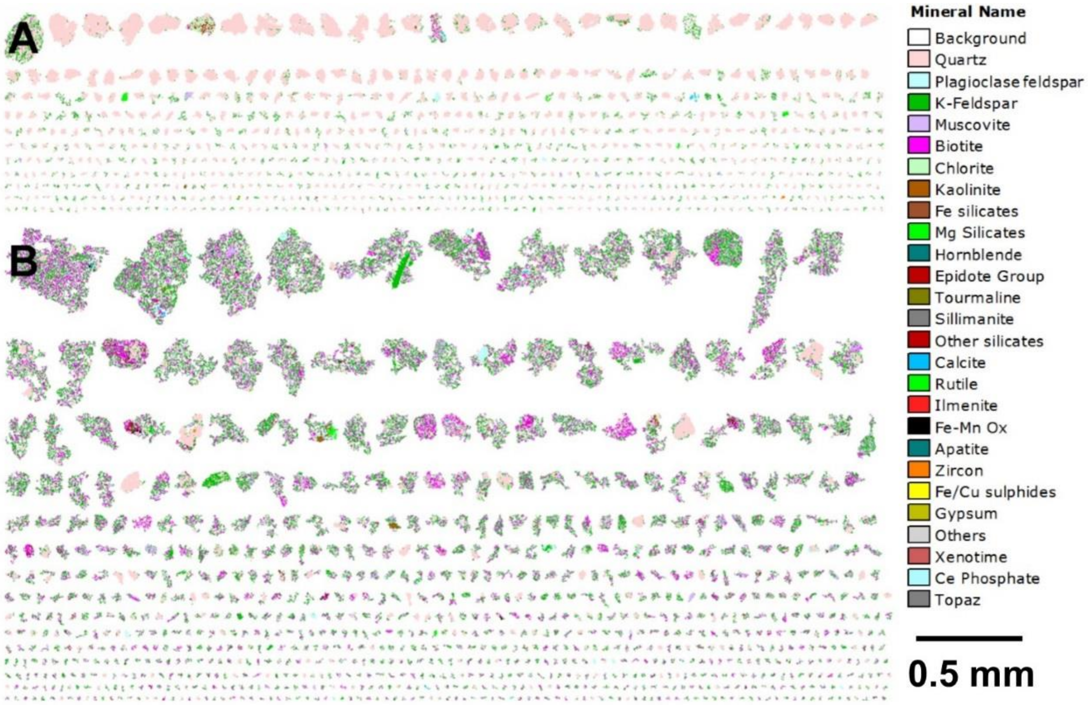

Figure 5

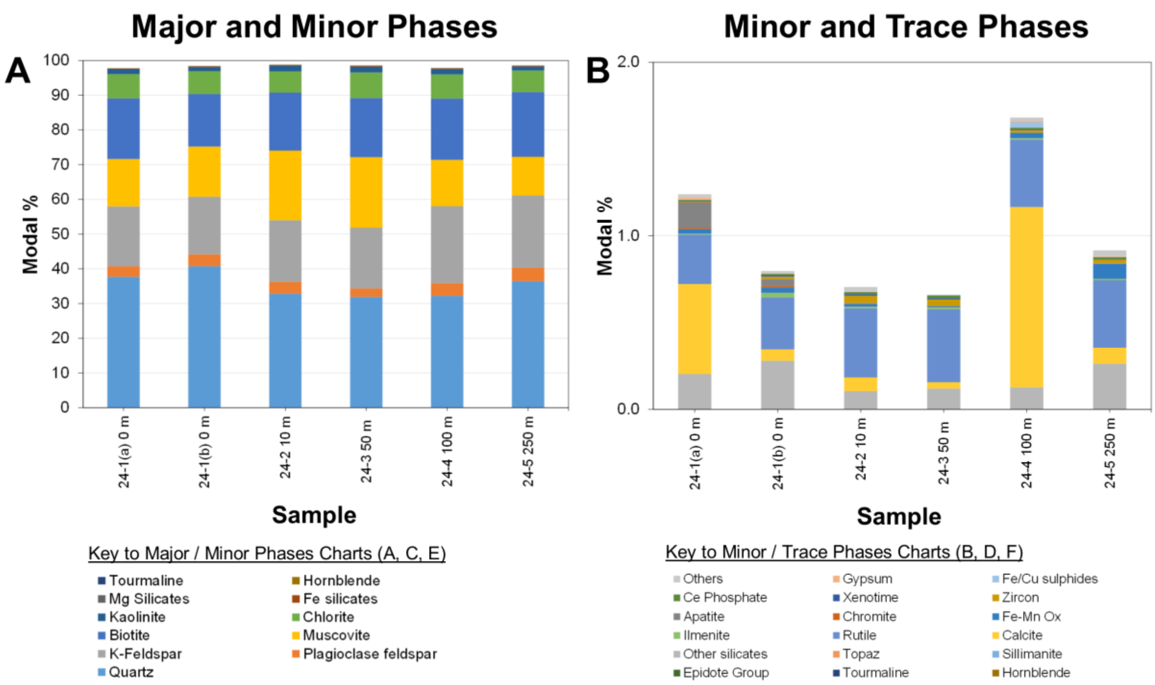

Figure 6

919 ***Table 1.*** *Sampling locations, bedrock geology, OS grid reference and land use.*

	Rock type	Formation	Age	Land use	Grid Reference
1/1	Granite	Lands End Granite	Permian	Resown grassland	SW45821 25934
2/1	Dolerite	Dolerite	Devonian	Pasture	SW54743 29115
3/1	Granite	Tregonning-Godolphin Granite	Permian	Managed grassland	SW60211 27618
4/1	Gneiss	Kennack Gneiss	Devonian (?Famennian)	Managed grassland	SW72090 16757
5/1	Mica schist	Old Lizard Head Formation	?Cambrian	Managed grassland	SW80076 22399
6/1	Meta-mudstone	Dartmouth Group	Devonian (Lochkovian-Pragian)	Pasture	SX14051 53330
7/1	Meta-mudstone	Meadfoot Group	Devonian (Pragian-Emsian)	Crops - maize	SX15377 58140
8/1	Meta-mudstone	Saltash Formation	Devonian-Carboniferous (Emsian-Tournasian)	Resown grassland	SX15571 63977
9/1	Meta-sandstone	Staddon Formation	Devonian (Emsian)	Pasture (very wet)	SX13368 63620
10/1	Granite	St Austell Granite	Permian-Carboniferous	Crops - maize	SX05528 56036
11/1	Meta-sandstone / mudstone	Dodman Formation	Early Devonian	Pasture	SX00095 40220
12/1	Dolerite	Nare Head Dolerite	Devonian (Givetian-Frasnian)	Managed grassland	SW92165 37879
13/1	Meta-mudstone	Roseland Breccia Formation	Devonian (Givetian-Frasnian)	Managed grassland (wet)	SW74187 24719
14/1	Schist	Traboe Hornblende Schist (Traboe Cumulate Complex)	Devonian (?Emsian)	Managed grassland	SW 74614 21750
15/1	Gabbro	Trelan and Crousa Gabbro	Devonian	Managed grassland	SW77884 21082
16/1	Serpentinite	Lizard Serpentinite	Devonian (Emsian) (mantle exhumation)	Managed grassland	SW77486 18004
17/1	Granite	Carnmenellis Granite	Permian	Managed grassland	SW72821 34663
18/1	Meta-mudstone	Mylor Slate Formation	Devonian (Frasnian-Famennian)	Managed grassland	SW80249 37757
19/1	Meta-mudstone	Trevose Slate Formation	Devonian (Frasnian-Famennian)	Managed grassland	SX07049 77239
20/1	Granite	Bodmin Granite	Permian	Moorland (grazed)	SX10137 78066
21/1	Meta-mudstone	Tredorn Slate Formation	Devonian (Famennian)	Managed grassland	SX07053 85000
22/1	Basaltic calcareous tuffs	Tintagel Volcanic Formation	Carboniferous (Visean)	Coastal grassland	SX04879 86451
23/1	Meta-mudstone	Polzeath Slate Formation	Devonian (Frasnian-Famennian)	Managed grassland	SW96717 77740
24/1	Meta-mudstone	Porthtowan Formation	Devonian (Eifelian-Frasnian)	Grassland margin to cultivated field	SW78531 47936
25/1	Meta-sandstone / mudstone	Portscatho Formation	Devonian (Givetian-Frasnian)	Managed grassland	SW71594 24780
26/1	Meta-mudstone	Bovisand Formation	Devonian (Pragian-Emsian)	Managed grassland	SX23501 58986
27/1	Meta-mudstone	Whitsand Bay Formation	Devonian (Lochkovian-Pragian)	Managed grassland	SX33649 54060
28/1	Meta-mudstone	Torpoint Formation	Devonian (Frasnian-Famennian)	Managed grassland	SX39086 57333
29/1	Meta-mudstone	Tavy Formation	Devonian (Frasnian-Famennian)	Grazed pastureland	SX40710 63197
30/1	Chert	Teign (Newton) Chert Formation	Carboniferous (Visean)	Grassland margin to cultivated field	SX34764 64914
31/1	Mudstone	Brendon Formation	Carboniferous (Visean)	Managed grassland	SX38587 68631
32/1	Basalt-Mudstone	Milton Abbott Formation	Carboniferous (Visean)	Managed grassland	SX45785 77497
33/1	Sandstone-Mudstone	Bealsmill Formation	Carboniferous (Serpukhovian-Bashkirian)	Moorland (near to Wheal Betsy mine)	SX50899 81429
34/1	Dolerite	Dolertie	Devonian-Carboniferous	Moorland (grazed)	SX52403 80699
35/1	Granite	Dartmoor Granite	Permian	Moorland	SX55354 75059

Table 2. *Soil sample numbers, laboratory codes, number of particles measured and number of individual EDS analyses.*

Sample	Block Code	Number of particles	Number of EDS analyses
1/1	16HG31	5017	170581
2/1	16HG32	5087	340966
3/1	16HG33	5257	95018
4/1	16HG34	5159	183139
5/1	16HG35	5009	179889
6/1	16HG36	5348	144111
7/1	16HG37	5051	487685
8/1	16HG38	5065	344579
9/1	16HG39	5362	60501
10/1	16HG3A	5249	199123
11/1	16HG3B	5152	200560
12/1	16HG3C	5077	214346
13/1	16HG3D	5060	153689
14/1	16HG3E	5570	144240
15/1	16HG3F	5109	121620
16/1	16HG3G	5170	98969
17/1	16HG3H	5148	72579
18/1	16HG3I	5145	109501
19/1	16HG3J	5210	89146
20/1	16HG3K	5392	73202
21/1	16HG3L	5280	60674
22/1	16HG3M	5257	73762
23/1	16HG3N	5080	325097
24/1	16HG3O	5385	113463
25/1	16HG3P	5304	117203
26/1	16HG3Q	5021	102166
27/1	16HG3R	5105	112770
28/1	16HG3S	5191	172621
29/1	16HG3T	5197	135687
30/1	16HG3U	5087	197134
31/1	16HG3V	5645	62752
32/1	16HG3W	5524	110229
33/1	16HG3X	5075	50734
34/1	16HG3Y	5098	81299
35/1	16HG3Z	5220	77215
24/1	16HG3AA	5213	95367
24/2	16HG3AB	5057	67539
24/3	16HG3AC	5066	87886
24/4	16HG3AD	5075	119598
24/5	16HG3AE	5123	107509

Table 3. *Mineral groupings used to process automated mineralogy data.*

Mineral Grouping	Description
Quartz	Quartz. May include other silica minerals
Plagioclase feldspar	Plagioclase (albite to anorthite solid solution)
K feldspar	K feldspar such as orthoclase and microcline
Muscovite	Muscovite. May include alteration products after feldspars such as sericite. Illite also reports to this category.
Biotite	Biotite and phlogopite. Would also include glauconite
Chlorite	Chlorite. Man-made slags would also report to this category
Kaolinite	Kaolinite, halloysite. dickite
Fe silicates	Nontronite and other Fe silicates
Mg silicates	Mg silicates such as serpentine group minerals, orthopyroxene, olivine
Hornblende	Hornblende and other amphiboles
Tourmaline	Tourmaline group minerals
Epidote Group	Epidote group minerals
Sillimanite	Sillimanite, andalusite, kyanite
Topaz	Topaz
Other silicates	Garnet. Al silicates
Calcite	Calcite, ankerite, dolomite, magnesite
Rutile	Rutile, titanite (sphene)
Ilmenite	Ilmenite
Fe-Mn Ox	Fe oxides (magnetite, hematite), Mn oxides
Chromite	Chrome spinel
Apatite	Apatite, biogenic apatite
Zircon	Zircon
Xenotime	Xenotime
Ce phosphate	Monazite
Fe / Cu sulphides	Pyrite, chalcopyrite
Gypsum	Gypsum
Others	Any other mineral not reported above

Table 4. *Modal mineralogical data for the 35 soil samples analysed throughout Cornwall and Devon, SW England.*

	1-1	2-1	3-1	4-1	5-1	6-1
Quartz	47.17	18.57	52.89	21.80	24.17	29.10
Plagioclase feldspar	9.38	9.06	10.39	17.45	13.24	4.80
K-Feldspar	19.18	7.36	16.95	13.71	10.05	26.77
Muscovite	2.44	1.11	3.82	0.90	2.26	8.21
Biotite	7.01	16.26	5.03	4.26	12.40	15.93
Chlorite	11.83	35.42	7.74	23.50	22.30	11.51
Kaolinite	0.84	0.29	1.71	0.08	3.18	1.30
Fe silicates	0.44	0.80	0.27	1.63	0.61	0.67
Mg Silicates	0.02	0.12	0.00	11.05	0.11	0.01
Hornblende	0.19	2.56	0.01	4.31	2.62	0.02
Tourmaline	0.06	0.90	0.03	0.15	0.48	0.01
Epidote Group	0.51	1.52	0.65	0.02	5.97	0.34
Sillimanite	0.00	0.00	0.01	0.00	0.00	0.00
Topaz	0.01	0.00	0.01	0.00	0.00	0.00
Other silicates	0.15	1.86	0.07	0.31	1.39	0.25
Calcite	0.10	0.32	0.08	0.08	0.11	0.25
Rutile	0.45	1.77	0.19	0.26	0.70	0.52
Ilmenite	0.08	0.70	0.04	0.02	0.18	0.02
Fe-Mn Ox	0.08	0.60	0.01	0.32	0.15	0.13
Chromite	0.01	0.02	0.01	0.07	0.01	0.04
Apatite	0.00	0.69	0.01	0.06	0.01	0.04
Zircon	0.02	0.02	0.01	0.01	0.01	0.03
Xenotime	0.01	0.01	0.02	0.00	0.01	0.00
Ce Phosphate	0.00	0.00	0.00	0.00	0.00	0.00
Fe/Cu sulphides	0.01	0.00	0.00	0.00	0.00	0.01
Gypsum	0.00	0.01	0.00	0.00	0.00	0.00
Others	0.01	0.02	0.01	0.00	0.02	0.00

Table 5. *Key mineralogical parameters for the six granite derived soils compared with the classification of the exposed granite types from (Simons et al., 2016).*

	1 - Lands End Granite	3 - Tregonning Godolphin Granite	10 - St Austell Granite	17 - Carnmenellis Granite	20 - Bodmin Moor Granite	35 - Dartmoor Granite
Kfsp	19.18	16.95	18.62	22.39	29.09	39.31
Plag	9.38	10.39	8.89	8.79	19.33	11.11
Biot	7.01	5.03	6.22	4.21	1.30	4.88
Musc	2.44	3.82	7.87	4.47	4.47	3.70
Kaol	0.84	1.71	3.93	1.79	1.30	1.67
Tourm	0.51	0.65	2.40	0.52	1.00	1.58
Sillim	0	0.01	0.01	0.03	0.23	0
Topaz	0.01	0.01	0	0.02	0.21	0
Granite types	G3 biotite granite G4 tourmaline granite	G1 two mica granite G5 topaz granite	G3 biotite granite G4 tourmaline granite	G1 two mica granite G2 Muscovite granite	G1 two mica granite G2 Muscovite granite	G3 biotite granite G4 tourmaline granite

Table 6. *Modal mineralogical data for the soil samples collected along a 250 m transect at Location 24, near Allet, Truro, Cornwall, with replicate sample 24/1.*

	24-1(a) 0 m	**24-1(b) 0 m**	**24-2 10 m**	**24-3 50 m**	**24-4 100 m**	**24-5 250 m**
Quartz	37.69	40.77	32.84	31.91	32.20	36.42
Plagioclase feldspar	3.06	3.41	3.48	2.41	3.68	3.91
K-Feldspar	17.22	16.60	17.68	17.51	22.13	20.75
Muscovite	13.65	14.45	20.03	20.31	13.37	11.17
Biotite	17.49	15.12	16.71	17.05	17.67	18.66
Chlorite	7.00	6.58	6.11	7.38	6.98	6.23
Kaolinite	1.40	1.15	1.70	1.66	1.54	1.17
Fe silicates	0.25	0.26	0.18	0.31	0.22	0.21
Mg Silicates	0.01	0.00	0.05	0.00	0.01	0.03
Hornblende	0.01	0.00	0.01	0.00	0.03	0.05
Tourmaline	0.97	0.85	0.46	0.79	0.45	0.47
Epidote Group	0.02	0.01	0.00	0.00	0.03	0.02
Sillimanite	0.00	0.00	0.01	0.00	0.00	0.00
Topaz	0.00	0.00	0.02	0.00	0.00	0.00
Other silicates	0.20	0.28	0.10	0.12	0.13	0.26
Calcite	0.52	0.07	0.08	0.04	1.04	0.09
Rutile	0.29	0.30	0.40	0.42	0.39	0.39
Ilmenite	0.01	0.03	0.01	0.01	0.01	0.01
Fe-Mn Ox	0.03	0.03	0.02	0.01	0.03	0.09
Chromite	0.01	0.01	0.00	0.00	0.00	0.00
Apatite	0.15	0.04	0.00	0.00	0.00	0.00
Zircon	0.01	0.01	0.04	0.04	0.02	0.02
Xenotime	0.00	0.01	0.01	0.01	0.01	0.00
Ce Phosphate	0.01	0.01	0.01	0.01	0.01	0.01
Fe/Cu sulphides	0.00	0.00	0.00	0.00	0.03	0.00
Gypsum	0.01	0.00	0.00	0.00	0.01	0.01
Others	0.02	0.01	0.03	0.00	0.02	0.03

